Eksplorium *p*-ISSN 0854-1418
Volume 44 No. 1, May 2023: 1–12 *e*-ISSN 2503-426X

Tectonic Structures of Northern Sumatra Region Based on Seismic Tomography of P and S Wave Velocity

Betrix Elisabet Silitonga[1], Iman Suardi[2], Akmal Firmansyah[3], Muhammad Hanif[4], Mohamad Ramdhan[4]*, Andry Syaly Sembiring[3]
[1]Geophysics Station of Gunung Sitoli-BMKG,
Meteorologi St., Gunung Sitoli, Sumatera Utara, 22811, Indonesia
[2]Study Program of Geophysics, School of Meteorology, Climatology, and Geophysics of Indonesia (STMKG), Pondok Betung, Pondok Aren, Tangerang Selatan, Banten, 15221, Indonesia
[3]Center for Earthquake and Tsunami-BMKG,
Angkasa I St., Kemayoran, Jakarta, 10610, Indonesia
[4]Research Center for Geological Disaster-BRIN,
KST Samaun Samadikun, Sangkuriang St., Cisitu, Bandung, 40135, Indonesia
*E-mail: mohamad.ramdhan@brin.go.id

Article received: 11 January 2023, revised: 25 May 2023, accepted: 29 May 2023
DOI: 10.55981/eksplorium.2023.6784

ABSTRACT

The tectonic setting of Sumatra Island is strongly influenced by the oblique subduction of the Indo-Australian Plate, which subducts the Eurasian Plate at a speed of 52–60 mm/year. The movement of these plates resulted in the Northern Sumatra region having seismic sources from tectonic and volcanic activity. The data used in this study is in the form of seismic wave travel-time recorded by numerous seismic stations in the research area from January 2012 to December 2020. The data comes from 5,003 earthquakes recorded by the BMKG seismic network. The inversion is a simultaneous inversion between seismic velocity models (Vp and Vs) and hypocenter parameters by applying a double-difference seismic tomography algorithm. Tomogram results in parts of Aceh (Singkil and Subulussalam) and North Sumatra (Pakpak Bharat and Dairi) at a depth of 0 km show negative perturbations in Vp and Vs values and high Vp/Vs values. The anomaly is most likely related to cracks in fluid-saturated rocks. The tomograms in the south of Lake Toba at depths of 30 km and 40 km have high Vp and Vs perturbation values and low Vp/Vs values. This anomaly indicates a magma supply line that is no longer active or has cooled for a long time. Based on the seismic tomography modeling results, the subducted Indo-Australian Plate to the Eurasian Plate is visible in the study area.

Keywords: Northern Sumatera, seismic tomography, double difference, Vp, Vs, Vp/Vs.

INTRODUCTION

Northern Sumatra is one of the areas in Indonesia with high seismic activity. This activity originates from the island's subduction zones, active faults, and volcanic activity. These three seismic sources are strongly influenced by the movement of the Indo-Australian Plate, which tilts downward underneath the Eurasian Plate. The active Sumatran fault stretches for 1,900 km and comprises 19 segments [1].

Volcanic activity, which is relatively high on the island of Sumatra, occurs on Mount Sinabung. Eruptions on the mountain have been recorded at least eight times since 2010. The last eruption activity occurred on 8 August 2020. Previously, the last eruption of Mount Sinabung was recorded in 1600. On 27 August 2010, it became active again with the eruption of Mount Sinabung recorded by the Center for Volcanology and Geological Hazard Mitigation (PVMBG) [2],[3]. In

addition, the most volcanic activity on the island occurred 74,000 years ago in the form of an eruption of Mount Toba, which produced the Toba Caldera [4].

Research on tectonic diversity in Northern Sumatra needs to be carried out to mitigate earthquake disasters by knowing and understanding the subsurface tectonic structure. Tectonic studies of a region can be carried out by applying the seismic tomography method to earthquakes recorded at seismic stations around the study area. The method used in this study is the double difference seismic tomography (tomoDD) method. The inversion is a simultaneous inversion between P wave velocity (Vp), S wave velocity (Vs), and hypocenter parameters [5]. The Vp/Vs ratio value results from dividing the inversion Vp against the inversion Vs. These three parameters interpret the tectonic conditions under the Northern Sumatra region and its surroundings.

The input to the tomoDD application is the travel time for the propagation of earthquake waves that have been paired with other earthquakes using the ph2dt program [6]. In addition to earthquake travel-time data, an initial velocity model is also needed for the seismic tomographic inversion process. The quality of the modeling results depends on the quantity and quality of the earthquake data used. The more earthquake data and the denser the seismic stations used, the better the subsurface structure information obtained.

DATA AND METHODS

The research area is located in the northern part of Sumatra with coordinate boundaries of 92.6798° E, 1.1809° N; 99.3817° E, 5.9013° N; 102.0592° E, 2.0491° N; and 95.3604° E, 2.6713° S. Seismic wave arrival time data comes from 5,003 earthquakes for the period January 2012–December 2020 which were obtained from the earthquake catalog repository of the Meteorology, Climatology, and Geophysics Agency (BMKG).

The original data format is converted by a Python-based program into the *.pha file extension as input to the ph2dt program. This program performs pre-processing by pairing an earthquake with the surrounding earthquakes [6]. Then, the resulting output becomes an input to the tomoDD program [5].

The stages of model parameterization, which include determining nodes and velocity models, must be carried out before processing data in tomoDD. As shown in Figure 1, this study uses 15 x and z-axes nodes and nine y-axis nodes with an axis rotation of -35°. The distance between nodes on the x and y axes is 65 km with tie points at coordinates 97.37 °E and 1.616° N.

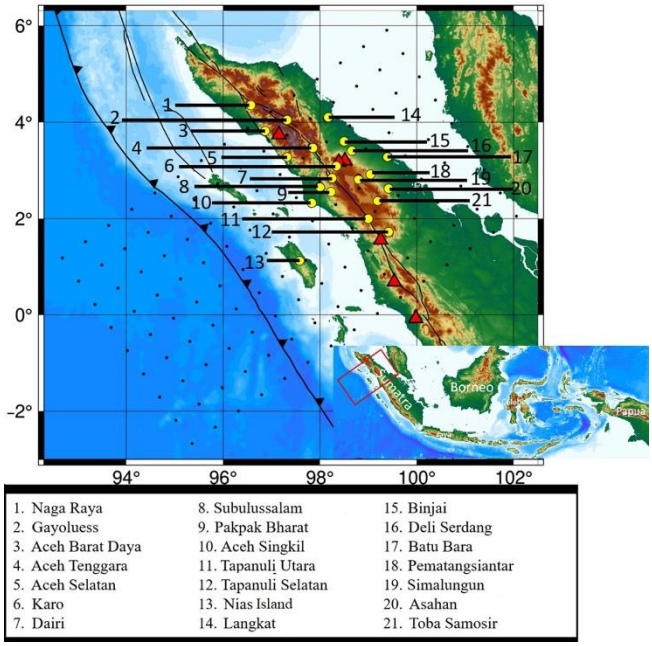

Figure 1. Distribution of nodes (black circles) used in the seismic tomographic inversion process. The red triangles indicate volcanoes. The red rectangle in the inset figure shows the position of the research area covered by grid nodes. Yellow circles represent regencies or cities in the study area. The subduction zone line and fault lines are taken from [7].

p-ISSN 0854-1418
e-ISSN 2503-426X

As shown in Table 1, the initial velocity model used is AK135 [8]. The inversion process on the model continues to be iterated until the final velocity model is reached, the state when the iteration process stops. The calculated seismic travel-time for the tomoDD application is formulated using the pseudo-bending method. According to Fermat's Principle, this method uses the fastest path from the earthquake source to the seismic station [9].

Table 1. AK135 velocity model [8].

Depth (km)	Vp (m/s)	Vs (m/s)
0.0	5.800	3.460
20.0	5.800	3.460
20.0	6.500	3.850
35.0	6.500	3.850
35.0	8.040	4.480
77.5	8.045	4.490
120.0	8.050	4.500
165.0	8.175	4.509
210.0	8.300	4.518

The inversion process produces several quantities: hypocenter parameters before relocation, hypocenter parameters after relocation, velocity models (Vp and Vs), residual travel-time for each station, and processing time. These results require validation, which can be done by looking at the conditional number of damping (CND) and root mean square (RMS) values. In addition, the inversion results can be validated by looking at the residual travel-time parameters. The seismic velocity results (Vp and Vs) obtained from the inversion process are mapped using perturbation values relative to the initial velocity input. In contrast, the value of Vp/Vs is plotted in absolute value. The seismic velocity inversion results were validated using the Derivative Weight Sum (DWS) method [10]. Previous studies have concluded that areas that can be interpreted correlate well with DWS scores of more than 500 [11].

RESULTS AND DISCUSSION

The pre-processing results with the ph2dt module show that 69% of the P phase and 72% of the S phase of the total data can be used as input in the tomoDD application. Validation of the hypocenter relocation results can be seen in Figure 2.

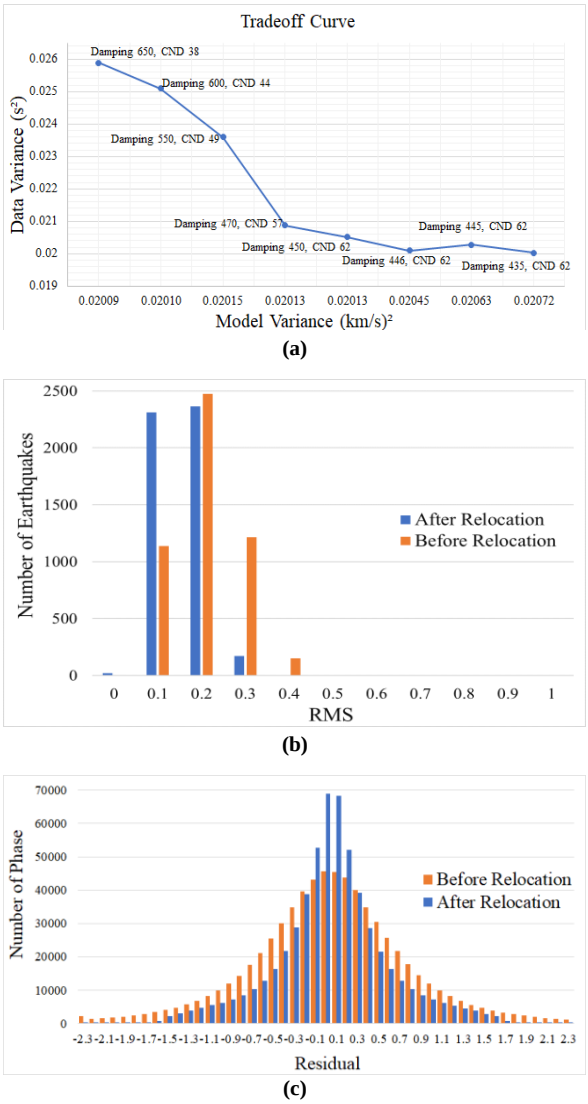

Figure 2. The trade-off curve to determine optimum damping (a). Comparison of RMS before and after relocation (b). Comparison of residual travel-time before and after hypocenter relocation (c).

Previous studies have shown that an excellent conditional amount of damping (CND) is between 40–80 [6],12]. This value indicates that the utilized damping value is not under or over-damping. This study obtained optimum results using a damping value of 450, resulting in a CND value of 62 (Figure 2a). On the other hand, compared to before relocation, the RMS after relocation result looks excellent, closer to 0 (zero) with the increasing number of earthquakes (Figure 2b). The validation of the residual inversion results of the travel-time of the earthquake wave phases (P and S phases) can also be categorized as good because there are more and more earthquake phases close to zero, as shown in Figure 2c. Thus, the earthquakes successfully relocated were 4,862 with their seismicity, as shown in Figure 3.

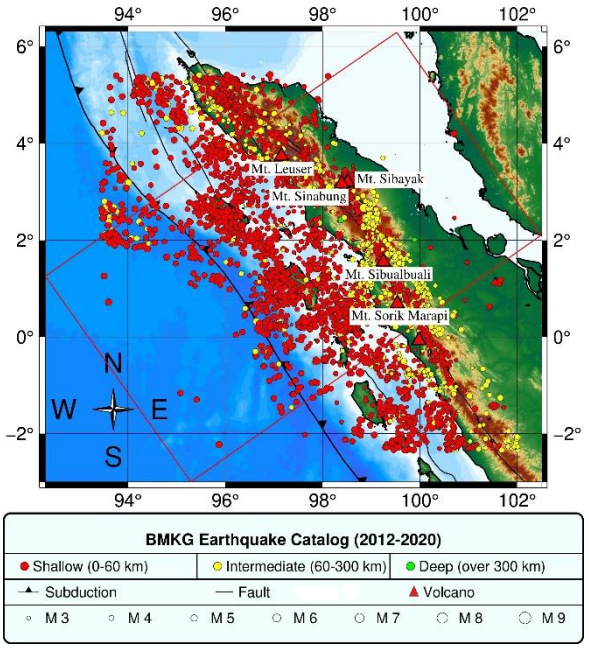

Figure 3. Earthquake distribution after hypocenter relocation.

Profile slicing was carried out on sections A-A', B-B', C-C', D-D', and E-E' perpendicular to the trench to see the vertical distribution of earthquakes (Figure 4). Changes in the hypocenter distribution after relocation are visible, especially in earthquakes with the same accumulation of depth to become more scattered (Figure 5).

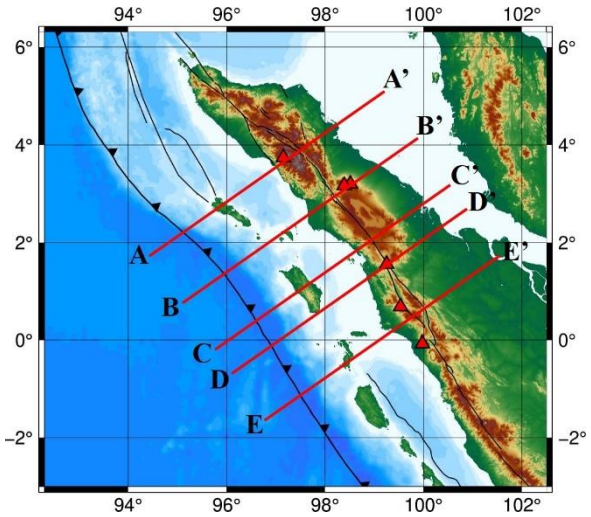

Figure 4. Cross sections A-A' to E-E', whose vertical sections can be seen in Figures 5 and 8.

The station density, the quantity of P and S wave phases, and the quality of the earthquake parameter results in the catalog affect the tomography results. The denser the stations and the more phases pass through a node, the better the resulting modeling. The quantity and quality of the P and S phase data will significantly affect the tomogram results produced [13]. The results of the horizontal tomogram and the Derivative Weight Sum (DWS) are shown in Figure 6 and Figure 7, while the results of the vertical tomogram of the slices and the DWS are shown in Figure 8 and Figure 9.

p-ISSN 0854-1418
e-ISSN 2503-426X

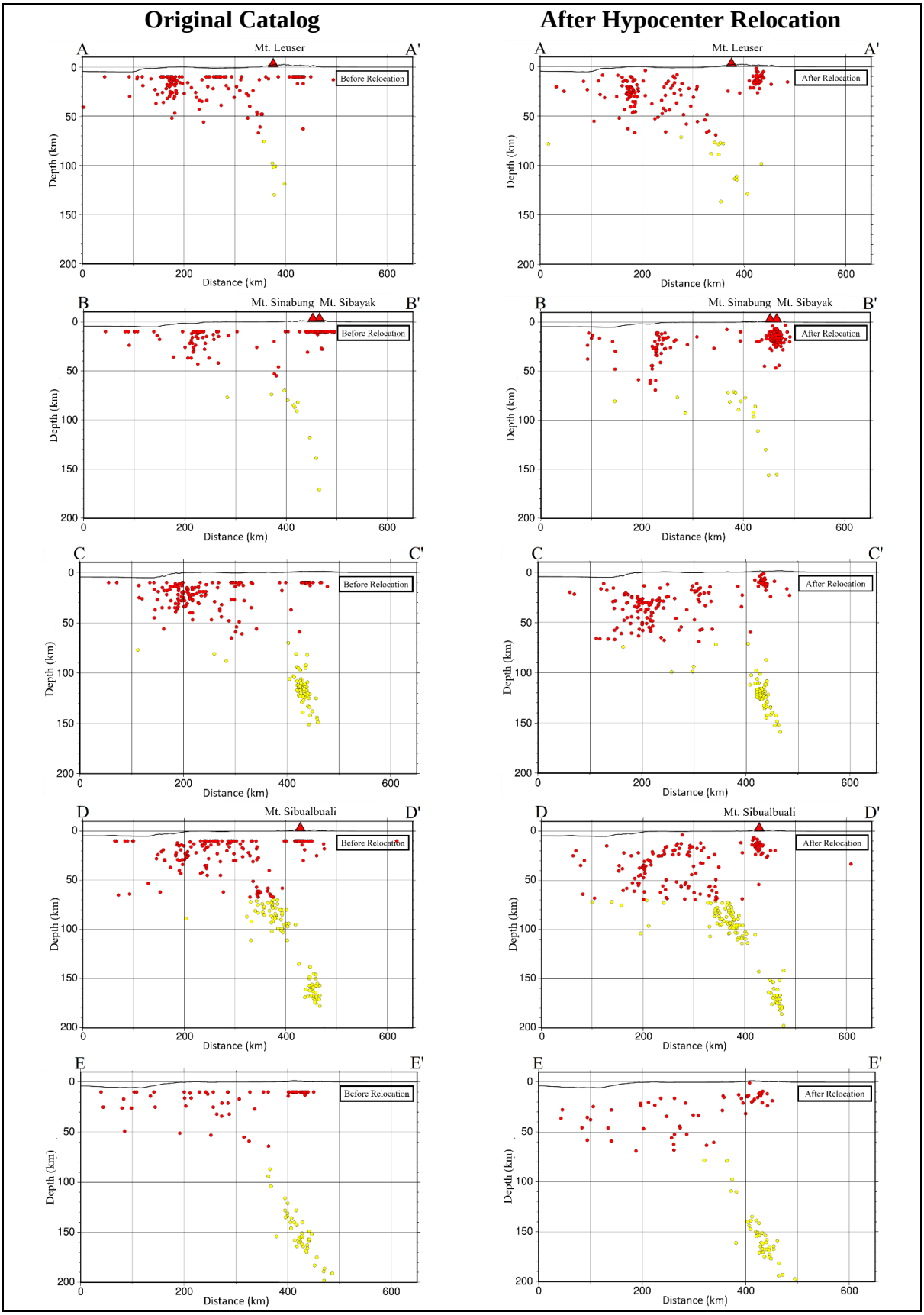

Figure 5. Vertical cross-section A-A' to E-E' before (left) and after hypocenter relocation (right). The red and yellow circles indicate hypocenter depths of less than and more than 60 km. The distance from the hypocenter (D) to the vertical cross-section line is -15 km ≤ D ≤ 15 km.

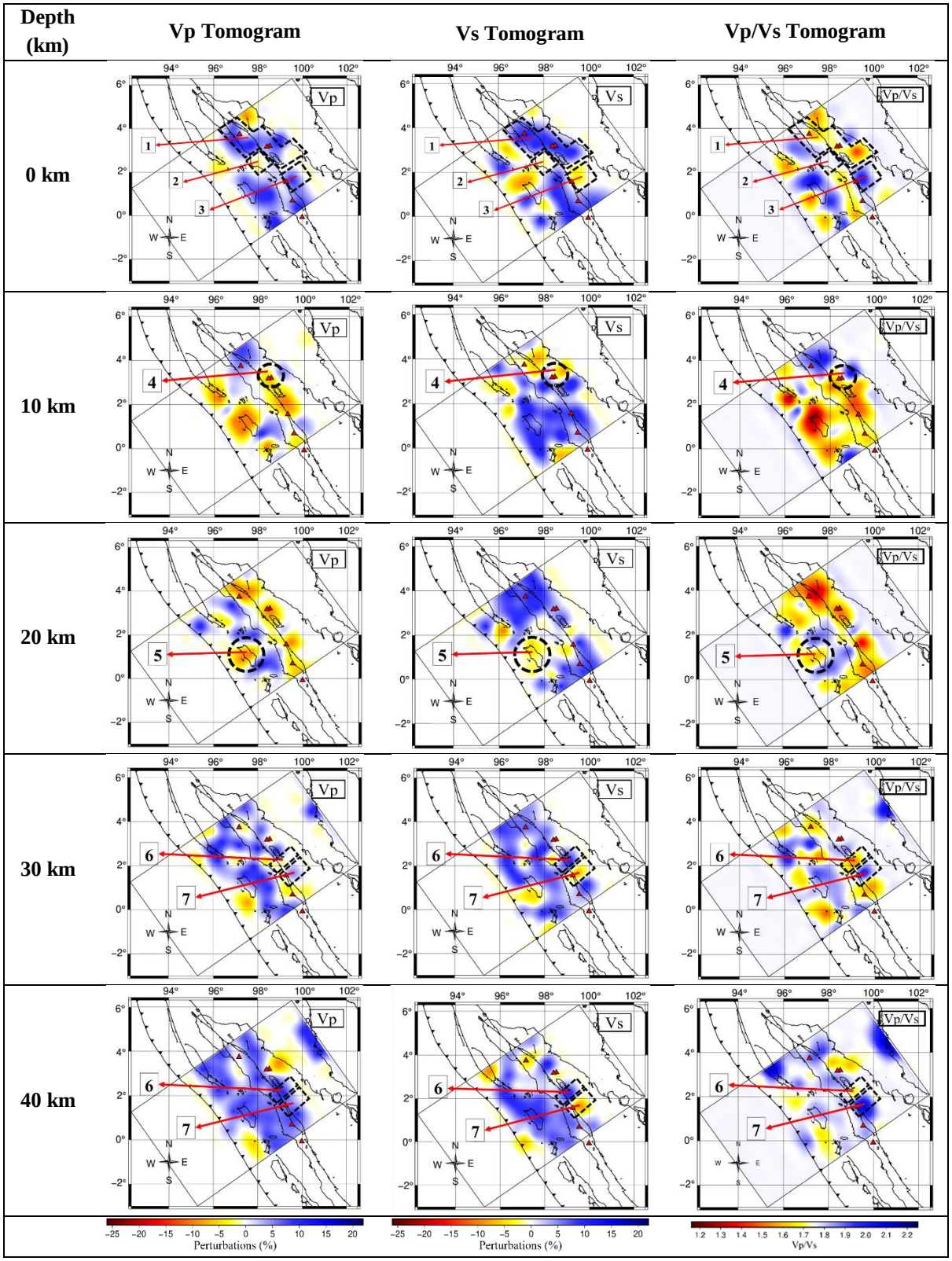

Figure 6. Horizontal tomograms at depths of 0–80 km for Vp (left), Vs (middle), and Vp/Vs (right). The dashed black line shows the interpretation of the anomaly indicated by the sequence of numbers. The DWS in Figure 7 represents areas that can be interpreted well, correlating with DWS values of more than 500 [11].

p-ISSN 0854-1418
e-ISSN 2503-426X

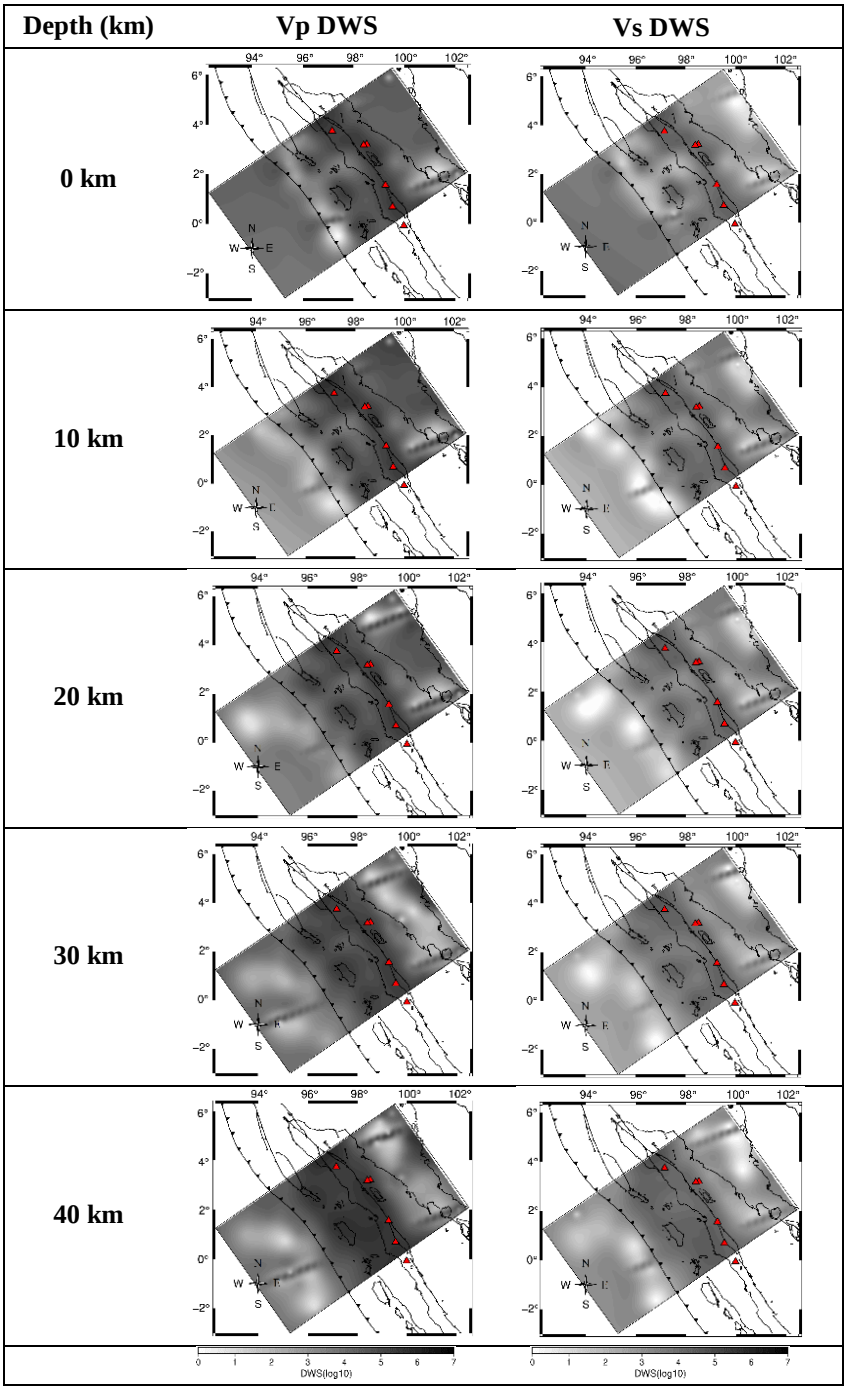

Figure 7. Derivative Weight Sum (DWS) at depths of 0–80 km for Vp (left) and Vs (right).

Anomaly Interpretation

We interpret the three anomalies at a depth of 0 km, as shown in Figure 6. The first interpretation (anomaly number 1) covers the Aceh region (Nagan Raya Regency, Southwest Aceh Regency, Gayo Lues Regency, South Aceh Regency, and Southeast Aceh Regency) and the North Sumatra region (Langkat Regency, Karo Regency, Binjai City, Deli Serdang Regency, Simalungun Regency, Pematangsiantar City, Batu Bara Regency, and Asahan Regency) which show high Vp and Vs perturbation values and low Vp/Vs. The anomaly indicates the presence of compact rock. The second interpretation (anomaly number 2) covers

some parts of the Aceh region (Aceh Singkil Regency and Subulussalam City) and North Sumatra (Pakpak Bharat Regency and Dairi Regency), which have low perturbation values of Vp and Vs and high Vp/Vs. This anomaly indicates the presence of sediment with a reasonably high fluid content [14]. The third interpretation is that in the south to southeast of Lake Toba (anomaly number 3), it has high Vp, low Vs, and high Vp/Vs perturbation values. The anomaly most likely indicates a crack in water-saturated rock [14].

The tomogram at a depth of 10 km is shown in Figure 6. Anomaly number 4 indicates an area with low Vp and Vs perturbation values and high Vp/Vs. This feature indicates the presence of fractures or weak zones filled with hot fluids [15]. At a depth of 20 km, the anomaly shows low perturbation values of Vp, Vs, and Vp/Vs on Nias Island (anomaly number 5). Nias Island results from sediment accumulation in the accretionary prism zone, causing a slowdown in the values of Vp and Vs [16].

High Vp and Vs perturbation values and low Vp/Vs values indicate a magma supply line that is no longer active and has cooled for a long time. High Vp and Vs perturbation values and low Vp/Vs can also indicate the presence of igneous intrusion [17]. The tomograms at 30 km and 40 km depth show structures with high Vp and Vs perturbation values and low Vp/Vs values. The anomaly is most likely related to the freezing of the magma path of Mount Toba (anomaly number 6). In addition, there are also rock structures filled with fluid, namely in South Tapanuli Regency, where the Vp and Vs perturbation values are low while the Vp/Vs is high (anomaly number 7).

Figure 8 shows the vertical section A-A' subduction zone model across Mount Leuser. Anomalies of high Vp and Vs and low Vp/Vs at a depth of 0-10 km around the mountain indicate the presence of bedrock structures in the area. The concentration of the earthquake hypocenter to the east of Mount Leuseur (black dashed line) on the vertical cross-section is thought to originate from the activity of the Tripa Segment, a segment of the Sumatran Fault.

The B-B' vertical cross-section in Figure 8 shows the accumulation of earthquake hypocenters underneath Mount Sinabung and Sibayak (circle dashed line). In addition, the cross-section passes through the Sumatra Fault in the Renun Segment. This hypocenter concentration is related to Mount Sinabung and the fault activities because the location of the two geological features is adjacent [1].

The hypocenter concentration on the C-C' section, marked by a black circle with a dashed line, originates from the Toru Segment activity (Figure 8). The hypocenter group, marked with a black circle with a dashed line on the D-D' section, is related to the Sumatran Fault segment originating from the Toru, Angkola, and Barumun Segments confluence. The D-D' cross-section also passes through Mount Sibualbuali. The E-E' section passes through the Sumatra Fault, which is identified as originating from the movement of the Angkola and Barumun Segments (black circle with dashed line). The entire cross-section shows that the Sumatran Fault zone is in a low Vp zone associated with an unstable zone [18].

Subduction zone modeling based on the tomogram of sections A-A' to E-E' (Figure 8) showed the steeper slab angle towards the south. This feature is related to the depth of the slab, which is deeper in that direction. Slab slopes are shown with high Vp and Vs anomalies associated with high density.

p-ISSN 0854-1418
e-ISSN 2503-426X

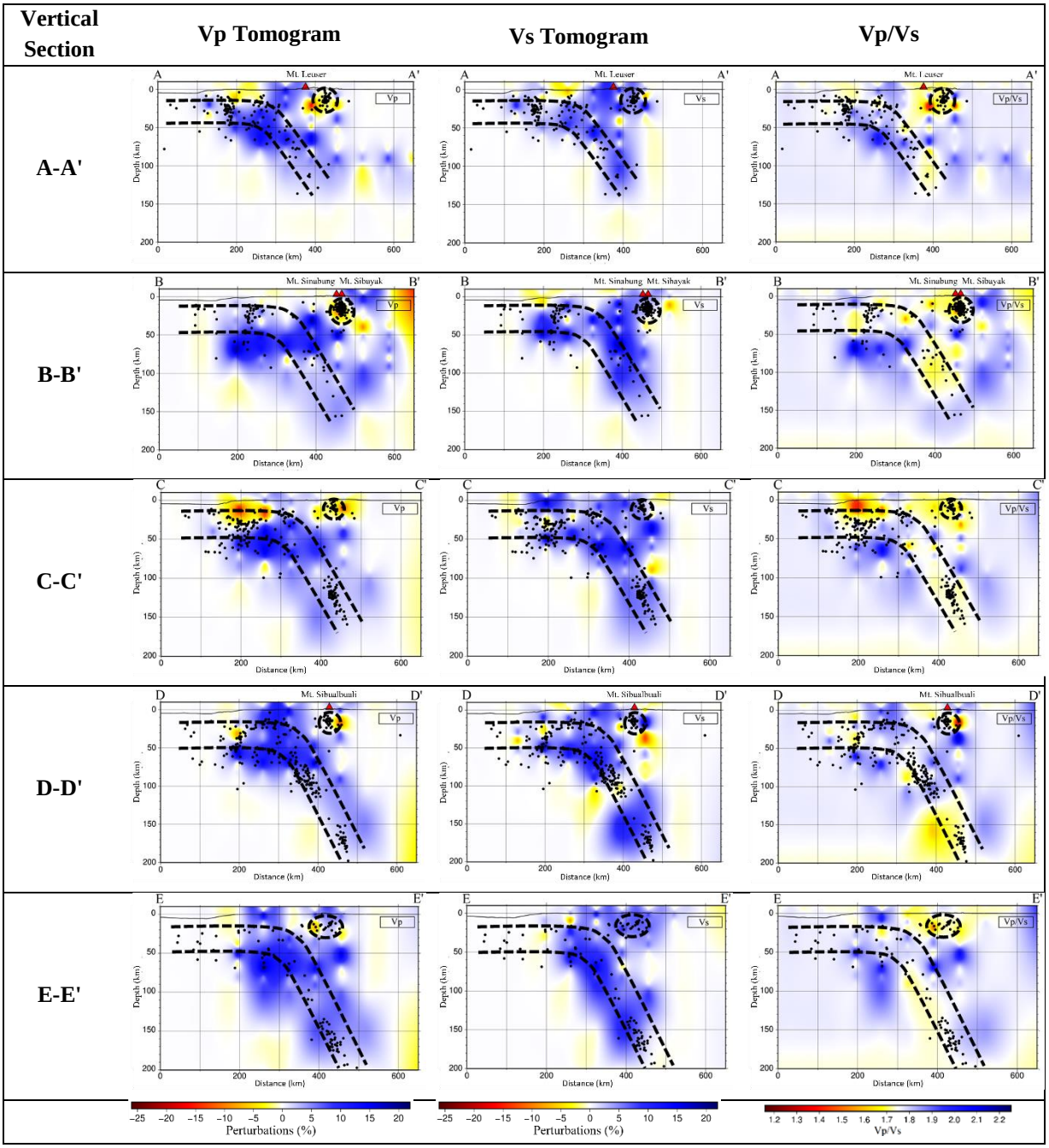

Figure 8. Vertical tomograms of Vp (left), Vs (right), and Vp/Vs (right) on the A-A' to E-E' sections. The Indo-Australian slab subducting the Eurasian Plate underneath the Northern Sumatra region and its surroundings is interpreted with dashed black lines. The black circles show the distribution of hypocenters, and circles with dashed black lines show the anomalies in the five sections. The areas that can be interpreted are depicted with the DWS scale in Figure 9.

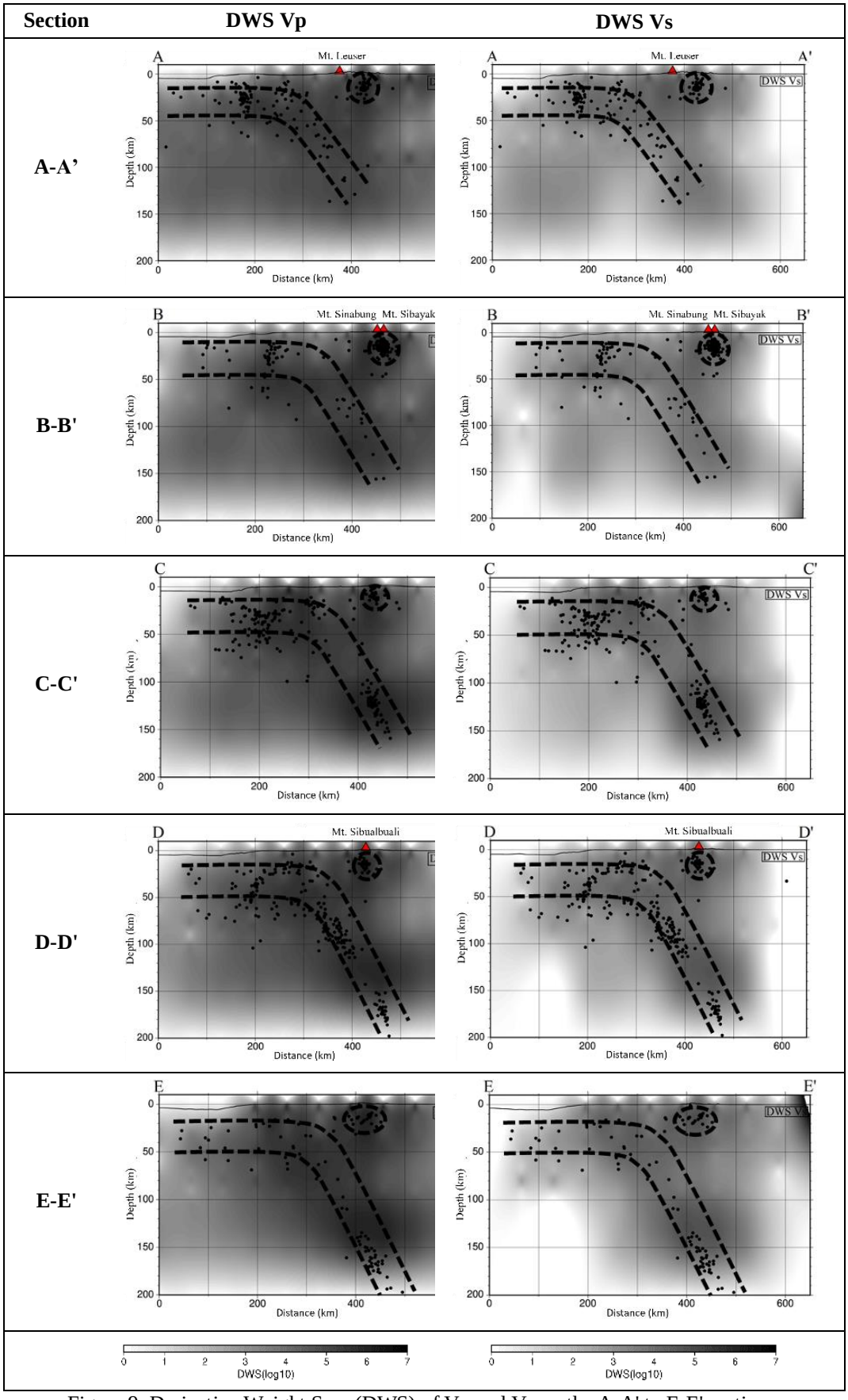

Figure 9. Derivative Weight Sum (DWS) of Vp and Vs on the A-A' to E-E' sections.

CONCLUSION

Modeling Northern Sumatra's tectonic structure using seismic tomography has yielded good results. Compact/rigid rock structures are mapped in Aceh and North Sumatra. Less compact structures, such as sediments, can be identified in the Aceh region (Aceh Singkil Regency and Subulussalam City) and North Sumatra (Pakpak Bharat Regency and Dairi Regency and Nias Island). The existence of low-velocity anomalies (low Vp and low Vs) and high Vp/Vs associated with fluids underneath Mount Sinabung, Mount Sibayak, and South Tapanuli Regency. Meanwhile, the rock structure with cracks saturated with water is modeled from the south to the southeastern part of Lake Toba. This study also showed clear subduction of the slab where the Indo-Australian Plate subducts under the Eurasian Plate, characterized by high values of Vp and Vs.

ACKNOWLEDGEMENTS

We express our deepest gratitude to the Center for Earthquake and Tsunami (PGT) Indonesian Agency for Meteorology, Climatology, and Geophysics (BMKG) for providing access to the earthquake catalog we need for this study.

AUTHOR CONTRIBUTIONS

All listed authors have contributed substantially to data processing, interpretation, and manuscript preparation and are the main contributors.

REFERENCES

[1] K. Sieh and D. Natawidjaja, "Neotectonics of the Sumatran fault, Indonesia," *Journal of Geophysical Research: Solid Earth*, vol. 105, no. B12, pp. 28295–28326, 2000, doi: 10.1029/2000JB900120.

[2] Ministry of Energy and Mineral Resources of the Republic of Indonesia, "Letusan G. Sinabung Kini Mirip Letusan 1.200 Tahun Lalu," *MEMR Media Center*, 21 January 2014, [Online]. Available: https://www.esdm.go.id/id/media-center/arsip-berita/letusan-g-sinabung-kini-mirip-letusan-1200-tahun-lalu (accessed 10 January 2023).

[3] Phys.org, "Volcano Quiet for 400 Years Erupts in Indonesia," *Earth Sciences News*, 29 August 2010, [Online]. Available: https://phys.org/news/2010-08-volcano-quiet-years-erupts-indonesia.html (accessed 10 January 2023).

[4] C. A. Chesner and W. I. Rose, "Stratigraphy of the Toba Tuffs and the Evolution of the Toba Caldera Complex, Sumatra, Indonesia," *Bulletin of Volcanology*, vol. 53, no. 5, pp. 343–356, Jun. 1991, doi: 10.1007/BF00280226.

[5] H. Zhang and C. H. Thurber, "Double-difference Tomography: The Method and Its Application to the Hayward Fault, California," *Bulletin of the Seismological Society of America*, vol. 93, no. 5, pp. 1875–1889, 2003, doi: 10.1785/0120020190.

[6] F. Waldhauser, "HypoDD: A Program to Compute Double-difference Hypocenter Location," *US Geol. Surv. Openfile report*, pp. 01–113, 2001, doi: 10.3133/OFR01113.

[7] M. Irsyam et al., *Peta Sumber dan Bahaya Gempa Indonesia Tahun 2017*, Pusat Penelitian dan Pengembangan Perumahan dan Permukiman, Badan penelitian dan Pengembangan, Kementerian Pekerjaan Umum dan Perumahan Rakyat (in Indonesian), 2017.

[8] B. L. N. Kennett, E. R. Engdahl, and R. Buland, "Constraints on Seismic Velocities in the Earth from Travel-times," *Geophysical Journal International*, vol. 122, no. 1, pp. 108–124, Jul. 1995, doi: 10.1111/j.1365-246X.1995.tb03540.x.

[9] J. Um and C. Thurber, "A Fast Algorithm for Two-Point Seismic Ray Tracing," *Bulletin of the Seismological Society of America*, vol. 77, no. 3, pp. 972–986, 1987, doi: 10.1785/BSSA0770030972.

[10] D. Toomey and G. Foulger, "Tomographic Inversion of Local Earthquake Data from The Hengill-Grensdalur Central Volcano Complex, Iceland," *Journal of Geophysical Research: Solid Earth*, vol. 94, no. B12, pp. 17497–17510, 1989, doi: 10.1029/JB094iB12p17497.

[11] H. Zhang and C. Thurber, "Development and Applications of Double-difference Seismic Tomography," *Pure and Applied Geophysics*, vol. 163, no. 2, pp. 373–403, Mar. 2006, doi: 10.1007/s00024-005-0021-y.

[12] S. Rosalia, S. Widiyantoro, A. D. Nugraha, and P. Supendi, "Double-difference Tomography of P- and S-Wave Velocity Structure Beneath The Western Part of Java, Indonesia," *Earthquake*

Science, vol. 32, no. 1, pp. 12–25, 2019, doi: 10.29382/eqs-2019-0012-2.

[13] M. Ramdhan et al., "Detailed Seismic Imaging of Merapi Volcano, Indonesia, From Local Earthquake Travel-Time Tomography," *Journal of Asian Earth Sciences*, vol. 177, pp. 134–145, Jun. 2019, doi: 10.1016/j.jseaes.2019.03.018.

[14] M. Laigle et al., "Mount Etna Dense Array Local Earthquake P and S Tomography and Implications for Volcanic Plumbing," *Journal of Geophysical Research: Solid Earth*, vol. 105, no. B9, pp. 21633–21646, 2000, doi: 10.1029/2000JB900190.

[15] N. Indrastuti et al., "3-D Seismic Tomographic study of Sinabung Volcano, Northern Sumatra, Indonesia, During the Inter-eruptive Period October 2010–July 2013," *Journal of Volcanology and Geothermal Research*, vol. 382, pp. 197–209, Sep. 2019, doi: 10.1016/j.jvolgeores.2019.03.001.

[16] A. J. Barber, M. J. Crow, and J. S. Milsom, *Sumatra: Geology, Resources and Tectonic Evolution*, Geological Society of London, 2005, doi: 10.1144/GSL.MEM.2005.031.

[17] H. R. Smyth, R. Hall, and G. J. Nichols, *Cenozoic Volcanic Arc History of East Java, Indonesia: The Stratigraphic Record of Eruptions on an Active Continental Margin*, in: Formation and Applications of the Sedimentary Record in Arc Collision Zones, Geological Society of America Special Papers, vol. 436, A. E. Draut, P. D. Clift, and D. W. Scholl (Eds), Geological Society of America, 2008, pp. 199–222, 2008, doi: 10.1130/2008.2436(10).

[18] A. D. Nugraha, S. Ohmi, J. Mori, and T. Shibutani, "High Resolution Seismic Velocity Structure Around the Yamasaki Fault Zone of Southwest Japan as Revealed from Travel-Time Tomography," *Earth, Planets and Space*, vol. 65, no. 8, pp. 871–881, 2013, doi:10.5047/eps.2012.12.004.